Krylov Subspace Model Order Reduction for Aircraft Cabin Noise Investigation

Julius Schultz[1], Christopher Blech[2], Ulrich Römer[1], Matthias Bollhöfer[3] und Sabine C. Langer[2]
[1] *Technische Universität Braunschweig, Institut für Dynamik und Schwingungen, Email: j.schultz@tu-braunschweig.de*
[2] *Technische Universität Braunschweig, Institut für Akustik*
[3] *Technische Universität Braunschweig, Institut für Numerische Mathematik*

Introduction

Within the next decades, the number of flights is expected to increase further on, leading to more and more people exposed to cabin noise during flights. Noise levels are known to be a major factor correlating with health and well-being of the passengers and the crew. For the development of future aircraft, an analysis of sound pressure levels inside the passenger cabin with mechanical models may help to avoid high noise levels by novel technologies. Furthermore, the knowledge of wave propagations through the aircraft structure serves as information basis for the placement and effectiveness of smart noise reduction measures. In this work, an existing model of a generic aircraft fuselage segment considering all crucial parts like the outer skin, frames and the interior lining is applied to analyse sound pressure levels in the passenger cabin. A wave-resolving finite element approach then leads to a large linear system

$$\left(\underline{\mathbf{K}} - \omega^2 \mathbf{M}\right) \underline{\mathbf{x}} = \underline{\mathbf{f}}, \tag{1}$$

containing fluid and structural domains. In (1), $\underline{\mathbf{K}}$ is the complex stiffness matrix [1] including structural damping, $\mathbf{M}$ is the mass matrix and ω is the angular frequency.

Solving such a linear system under specific excitation $\underline{\mathbf{f}}$ many times to determine frequency response functions $\underline{\mathbf{x}}$ or even perform parameter studies is computationally challenging. Especially in early design phases, numerous uncertainties exist in the model parameters or the geometry, optimisation may be conducted or design studies are planned. All iterations in design require several solutions of the model. Hence, in this work, moment-matching model order reduction (MOR) methods, specifically, Krylov-based model order reduction (KMOR) methods are investigated in order to reduce the computational costs. A separate application of KMOR to (a) a plate structure and (b) a fluid volume is conducted delivering helpful findings about the method. Finally, KMOR is successfully applied to the generic aircraft segment with all structural and fluid domains gaining a drastic reduction of computational costs.

Projection-based model order reduction

The idea of projection based MOR is to describe the evolution of the system variable $\mathbf{x}(\omega) \in \mathbb{R}^n$ from (1) in a lower dimensional subspace of dimension $r \ll n$. By defining a matrix $\mathbf{V} \in \mathbb{R}^{n\times r}$ which spans the space $\mathcal{L} = \text{range}(\mathbf{V})$, one can define the approximation

$$\mathbf{x}(\omega) \approx \mathbf{V}\mathbf{x}_r(\omega)\,. \tag{2}$$

Substituting (2) into (1) gives rise to a residual

$$\mathbf{R}(\omega) = (-\omega^2\mathbf{M} + \mathbf{K})\mathbf{V}\mathbf{x_r}(\omega) - \mathbf{f}(\omega)\,. \tag{3}$$

The residual can be minimised by defining a r-dimensional trial space $\mathcal{J}$, with a corresponding matrix $\mathbf{W} \in \mathbb{R}^{n\times r}$ such that range$(\mathbf{W}) = \mathcal{J}$ and enforcing the Petrov-Galerkin condition

$$\mathbf{W}^T\mathbf{R} = 0\,. \tag{4}$$

A reduced order model (ROM) with system matrices of size $r \times r$ is constructed as

$$(-\omega^2\mathbf{M}_r + \mathbf{K}_r)\mathbf{x}_r = \mathbf{f}_r \tag{5}$$

with corresponding reduced matrices

$$\mathbf{M}_r = \mathbf{W}^T\mathbf{M}\mathbf{V},\ \mathbf{K}_r = \mathbf{W}^T\mathbf{K}\mathbf{V}, \mathbf{f}_r = \mathbf{W}^T\mathbf{f}\,. \tag{6}$$

Different choices of $\mathbf{V}$ and $\mathbf{W}$ lead to specific versions of reduced order modelling. In the next section the Krylov-based approach is explained in detail.

Krylov-based model order reduction

Originally, KMOR [1] has been developed for first order systems of the form

$$\begin{cases} s\mathbf{E}\mathbf{x}(s) & = \mathbf{A}\mathbf{x}(s) + \mathbf{B}\mathbf{u}(s) \\ \mathbf{y}(s) & = \mathbf{C}^T\mathbf{x}(s) \end{cases} \tag{7}$$

where $\mathbf{u} \in \mathbb{R}^m$ and $\mathbf{y} \in \mathbb{R}^p$ define the vector of m inputs and p outputs and $\mathbf{x} \in \mathbb{R}^n$ is the state variable, all depending on the Laplace variable s. The matrices $\mathbf{A} \in \mathbb{R}^{n\times n}$ and $\mathbf{E} \in \mathbb{R}^{n\times n}$ define system matrices and $\mathbf{B} \in \mathbb{R}^{n\times m}$ and $\mathbf{C} \in \mathbb{R}^{n\times p}$ define the input and output map, respectively. The corresponding transfer function reads

$$\mathbf{H}(s) = \mathbf{C}^T(s\mathbf{E} - \mathbf{A})^{-1}\mathbf{B}\,. \tag{8}$$

As highlighted in [2], the basic idea of KMOR is to determine a reduced order transfer function $\hat{\mathbf{H}}(s) = \hat{\mathbf{C}}^T(s\hat{\mathbf{E}} - \hat{\mathbf{A}})^{-1}\hat{\mathbf{B}}$ via projection, by

$$\hat{\mathbf{E}} = \mathbf{W}^T\mathbf{E}\mathbf{V},\ \hat{\mathbf{A}} = \mathbf{W}^T\mathbf{A}\mathbf{V},\ \hat{\mathbf{C}} = \mathbf{C}\mathbf{V},\ \hat{\mathbf{B}} = \mathbf{W}^T\mathbf{B} \tag{9}$$

that enforces a Hermite interpolation condition of $\mathbf{H}(s)$ and $\hat{\mathbf{H}}(s)$. This interpolation condition includes a certain number of derivatives (moments) at different interpolation points and is therefore referred to as moment-matching property. It reads

$$\frac{d^k}{ds^k}\mathbf{H}(s_i) = \frac{d^k}{ds^k}\hat{\mathbf{H}}(s_i) \tag{10}$$

[1] The underline indicating complex numbers is left out in all following equations for better readability.

for $k = 0, \ldots, q$ and $i = 0, \ldots, j$. Here, q denotes the number of moments matched and j refers to the number of interpolation points.

By defining the projection spaces $\mathbf{V}$ and $\mathbf{W}$ as Krylov subspaces

$$\mathcal{K}_q(\mathbf{A}, \mathbf{b}) = \mathrm{span}\{\mathbf{b}, \mathbf{Ab}, \mathbf{A}^2\mathbf{b}, \ldots, \mathbf{A}^{q-1}\mathbf{b}\} \tag{11}$$

a moment matching property can be achieved, following [1]: If the projection spaces are defined as

$$\mathrm{range}(\mathbf{V}) = \mathcal{K}_q(\tilde{\mathbf{A}}_0^{-1}\mathbf{E}, \tilde{\mathbf{A}}_0^{-1}\mathbf{B}) \tag{12}$$
$$\mathrm{range}(\mathbf{W}) = \mathcal{K}_q(\tilde{\mathbf{A}}_0^{-T}\mathbf{E}^T, \tilde{\mathbf{A}}_0^{-T}\mathbf{C}) \tag{13}$$
$$\text{with } \tilde{\mathbf{A}}_0 = \mathbf{A} - s_0\mathbf{E} \tag{14}$$

the first $2q$ moments of the original and reduced order transfer function match at the expansion point s_0. The theory can be extended to multi-point moment matching by concatenating multiple shifted Krylov subspaces for different shifts s_i such that

$$\bigcup_{i=1}^{j} \mathcal{K}_{q_i}(\tilde{\mathbf{A}}_i^{-1}\mathbf{E}, \tilde{\mathbf{A}}_i^{-1}\mathbf{B}) \subset \mathrm{range}(\mathbf{V}) \tag{15}$$
$$\bigcup_{i=1}^{j} \mathcal{K}_{q_i}(\tilde{\mathbf{A}}_i^{-T}\mathbf{E}^T, \tilde{\mathbf{A}}_i^{-T}\mathbf{C}) \subset \mathrm{range}(\mathbf{W}) \tag{16}$$

holds, where j denotes the number of expansion points.

In [2] and [3] the KMOR concept is transferred to second order dynamical systems. At first (1) is equipped with a input and output map $\mathbf{B}$ and $\mathbf{C}$

$$\begin{cases} (-\omega^2\mathbf{M} + \mathbf{K})\mathbf{x}(\omega) & = \mathbf{B}u(\omega) \\ y(\omega) & = \mathbf{C}^T\mathbf{x}(\omega) \end{cases} \tag{17}$$

In case of a single load, $\mathbf{B} \in \mathbb{R}^{n\times 1}$ is a vector that describes the distribution of the load and u just scales this distribution. For a single output, $\mathbf{C} \in \mathbb{R}^{n\times 1}$ is a vector as well and can be interpreted as a filter, that picks a certain node of interest or calculates some norm of the state variable.

To preserve the second order structure, the KMOR method is directly applied to the second order system. This approach leads to second order Krylov subspaces for the projection spaces that yield the desired moment matching property [3]. In the case of proportionally damped systems, it is shown in [3] that the second order Krylov subspace reduces to a first order Krylov subspace and the projection subspaces for the system (17) results in

$$\mathrm{range}(\mathbf{V}) = \mathcal{K}_q(\tilde{\mathbf{K}}_0^{-1}\mathbf{M}, \tilde{\mathbf{K}}_0^{-1}\mathbf{B}) \tag{18}$$
$$\mathrm{range}(\mathbf{W}) = \mathcal{K}_q(\tilde{\mathbf{K}}_0^{-T}\mathbf{M}^T, \tilde{\mathbf{K}}_0^{-T}\mathbf{C}), \tag{19}$$
$$\text{with } \tilde{\mathbf{K}}_0 = \mathbf{K} - \omega_0^2\mathbf{M}\,. \tag{20}$$

The space spanned by $\mathbf{V}$ is also called *input Krylov subspace* and the space spanned by $\mathbf{W}$ *output Krylov subspace*, since the first is build with the input map $\mathbf{B}$ and the latter with the output map $\mathbf{C}$. KMOR methods using both spaces are called two-side methods, while methods restricted to one space by setting $\mathbf{W} = \mathbf{V}$ are called one-side methods. One-side methods approximate the whole output space, since no output filter is required, however, come with the drawback of slower convergence, since less moments are matched.

It is well known, that the Krylov vectors converge to the eigenvector of the dominant eigenvalue of $\tilde{\mathbf{K}}^{-1}\mathbf{M}$ and therefore do not provide a stable basis. For practical implementation, numerical algorithms, like the Arnoldi algorithm are used to construct a numerical stable (i.e. orthonormal) basis of the defined Krylov subspaces. See [4] for more details.

Model properties

The aim of the paper is the investigation of KMOR methods for a generic aircraft fuselage model. A fuselage segment, originated from works of the Coordinated Research Center (CRC) 880 at TU Braunschweig is used as a reference model. The model includes the airframe (outer skin, frames, floor), the insulation, the interior cabin lining and the cabin fluid. In Fig 1, the different domains and the coupling interfaces are sketched. All domains are discretised by finite elements and 2D as well as 3D elements with quadratic ansatzfunctions are used. For further details of the model the reader is referred to [6]. For systematic investigation, the complex model is decomposed into its elementary submodels, describing the vibration of structures, sound propagation in fluids and the coupled vibro-acoustic problem. In Fig. 2, this approach is visualised by presenting the complex generic aircraft model and the derived simplified submodels. The KMOR algorithms are first applied to the elementary submodels and then used for MOR of the generic aircraft cabin model.

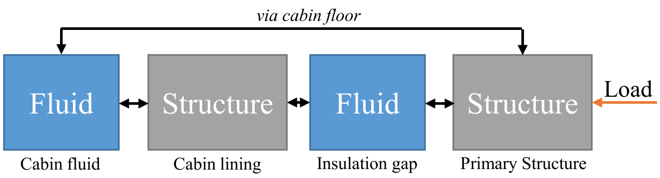

Figure 1: Sound-transmission path of the generic aircraft cabin model

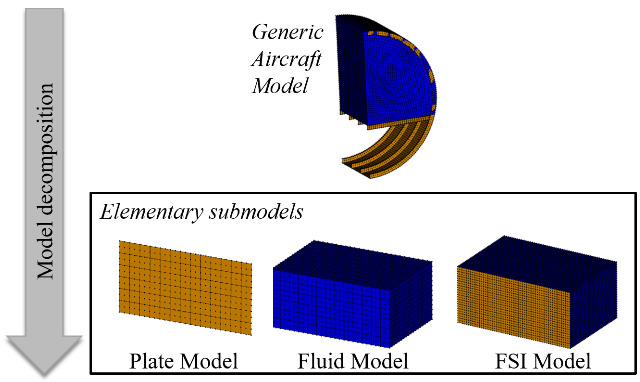

Figure 2: Overview of generic and application models

All models are investigated in a frequency range of $50-250$ Hz, the material of the structural model is aluminium and the medium of the fluid model is air. The discretisation is chosen such that a resolution of the smallest wave length is ensured. The submodels are constructed for different modal densities by adjusting the plate thickness or the size of the fluid cavity. The FSI model is constructed by combining the structural and fluid submodel.

Numerical Results

In this section the rational Krylov method based on the Arnoldi algorithm [1] is applied to the models presented in the last section. The accuracy of the ROM is determined by comparison against the full order model (FOM) solution. This is only practical for theoretical investigations, since in practise a FOM solution is often not affordable and once at hand a ROM solution is superfluous. However, error indicators are available which allow to efficiently assess the MOR error in large scale applications, see [7] for further details. Here, the maximum relative error over the entire frequency domain $\mathcal{F}$

$$\epsilon_{rel} = \max_{\omega \in \mathcal{F}} \frac{||\mathbf{y}(\omega) - \hat{\mathbf{y}}(\omega)||_\infty}{||\mathbf{y}(\omega)||_\infty} \tag{21}$$

is considered and required to be below a threshold of $\epsilon_{rel} < 1e-2$. In case of a one-side method, the output map $\mathbf{C}$ is chosen as the identity and consequently the error measure corresponds to a maximal global error, since all nodes are represented in the output vector $\mathbf{y}$. In case of a two-side method, that uses a SISO map, the output reduces to a scalar quantity and the corresponding error can be interpreted as a local quantity (error in the output node specified in the output map $\mathbf{c}$).

Once the accuracy requirement is verified, there are different possible performance measures of a ROM. One is the achieved speed-up of the total ROM computational time against the FOM calculation

$$s_{up} = \frac{t_{FOM}}{t_{ROM}} \, . \tag{22}$$

However s_{up} depends on the number of calculated samples and a very fine sampling of the frequency domain leads to a large speed-up. Another indicator is the final size of the ROM, which has to be much smaller than the FOM, since the sparsity of the FOM system is lost and the offline computational cost has to be paid off. Here, results for both performance measures are reported.

In the following it is explained how the ROM is constructed: The performance of the ROM depends on the chosen expansion points and the number of moments matched at these points. Keeping the number of expansion points low is beneficial, because each new expansion point requires the computation of a full size system factorisation (increasing off-line cost). However, the positive effect of adding moments reaches a saturation point.

The ROMs in this work are constructed manually by fixing the expansion points a priori and increasing the number of moments until the accuracy conditions are met. In Fig. 3, this process is demonstrated for the plate model by displaying the error of different ROMs around one expansion point $\omega_i = 150$ Hz. The ROM associated with

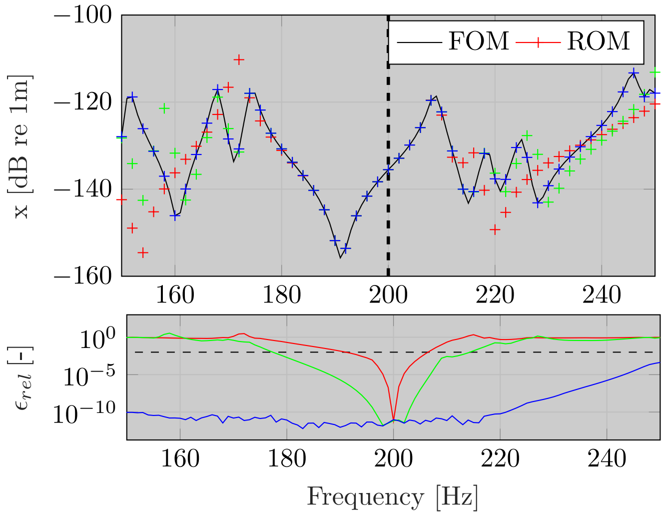

Figure 3: Top: Displacement at the excitation node of the model *Plate_a*. Bottom: Error analysis for three different ROMs (red, green, blue)

the red, the green and the blue line matches 5, 10 and 20 moments at the expansion point, respectively. For an increasing number of moments matched the converged region expands locally from the expansion point. For 20 moments matched (blue line) the ROM error ϵ_{rel} is below the defined threshold of 1e−2 in the whole considered frequency range. Note, that a different choice of expansion points might lead to an improved, i.e. smaller, ROM. However, in practical engineering applications it is often not important to find the smallest ROM. Instead, an accurate ROM is desired that yields a significant speed-up against the FOM computation.

The ROM performance results are summarized in Tab. 1 for the standardised submodels. The standardised models are investigated for different modal densities by adjusting the model properties like the plate thickness or the dimension of the fluid. For all models a frequency range from $50-250$ Hz with two expansion points at 100 Hz and 200Hz is considered.

Table 1: ROM performance summary

Model	Modes	Moments	$\frac{\text{ROM}}{\text{FOM}}$ size	Speed-up
Plate_a	17	20	42 / 3975	30
Plate_b	35	36	74 / 3975	18
Fluid_a	19	14	30 / 6669	53
Fluid_b	30	21	44 / 10881	45
FSI_a	36	36	74 / 56975	98
FSI_b	75	57	116 / 88775	97

At first it can be noticed, that an increasing modal density in the submodels, requires more moments to match and therefore leads to a larger ROM. Furthermore, the coupled model requires approximately the sum of the moments of the corresponding subsystems for an accurate

ROM. For all models the ROM size is at least two orders smaller than the FOM and the ROM size just increases linearly with the number of moments matched.

The speed-up value decreases for models with higher modal density, since the ROM size increases. Comparisons between the models show, that the plate models deliver the lowest speed-up values, while the FSI models yield the largest speed-up values. This is mainly related to the fact, that the FOM FSI problem is much more complex to solve for the direct solver, due to the higher bandwidth resulting from the coupling blocks.

Testing the KMOR method for the elementary submodels demonstrates the applicability for strongly coupled FSI models. However, applying the method to the generic aircraft model leads to a large ROM and therefore low speed-up values. The problem is the comparable high modal density, resulting from coupling modes of the four different domains and the requirement of the ROM to deliver an accurate ROM in all four domains. However, in some cases, only a small part of the domain is important, e.g. the sound pressure level at the passengers ear position. Under this condition, a two-side method can be applied, by additionally defining the output map $\mathbf{c}$, that specifies the relevant output nodes. Thus, *an accurate ROM is only constructed locally at a specified point.*

In Fig. 4, this local approximation property is shown by displaying the maximum relative error in the whole frequency domain for the different subdomains and for the locally defined point in the fluid domain.

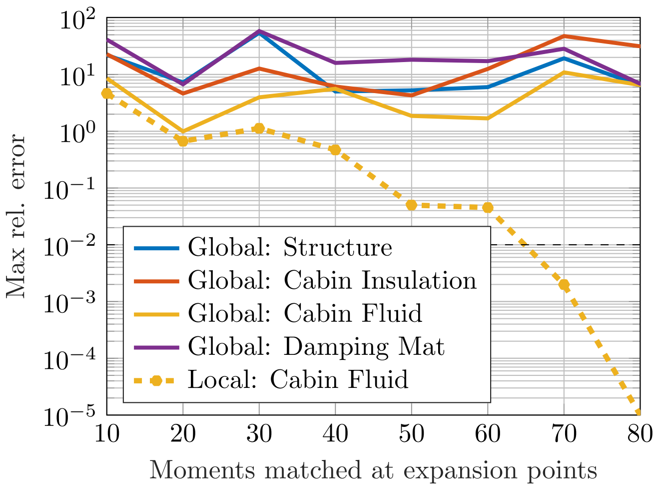

Figure 4: ROM error investigation for a two-side method of the generic aircraft model

As expected, the ROM converges only locally for the specified node in the fluid domain. This result is very promising, since it enables to reduce complex models by simply focusing on the relevant output nodes.

Conclusion and outlook

In this paper the applicability of KMOR methods for aircraft cabin noise investigations is systematically analysed. It is shown that KMOR methods deliver accurate and small ROMs for all generic models, i.e. the coupled FSI model and its submodels. Depending on the model, the final ROM size is decreased by factors of 10^2 to 10^3. This significant reduction of the problem size results in a very fast evaluation of the FRF, which is required for the acoustical design process. Application of the method to a generic aircraft model underlines, that two side methods are necessary to obtain small ROMs. These methods reduce the error at specified output nodes only and yield a local convergence property.

Furthermore, a correlation of the ROM size and the modal density of the models is shown. A higher modal density requires a larger projection space to obtain an accurate ROM. This observation is a promising approach to select the location of expansion points.

A big advantage of KMOR compared to standard MOR methods, like modal analysis, is the availability of error indicators. Based on these error indicators accurate ROMs can be constructed without computing the FOM reference solution, see [7].

Furthermore KMOR methods are extendible to so called *parametrised* MOR methods, which yield a valid ROM for variations in a multi-dimensional parameter space. In a first attempt the algorithm presented in [5] is applied to simple plate models. Handling high-dimensional parametric MOR problems and avoiding the *curse of dimensionality*, will be the scope of future research.

J.Schultz, U. Römer and S. C. Langer acknowledge the funding by the Deutsche Forschungsgemeinschaft (DFG, German Research Foundation) under Germany's Excellence Strategy – EXC 2163/1- Sustainable and Energy Efficient Aviation – Project-ID 390881007.

References

[1] Grimme, E.: "Krylov projection methods for model reduction", Doctoral dissertation, 1997.

[2] Beattie, C. A., Gugercin, S.: "Krylov-based model reduction of second-order systems with proportional damping", Proceedings of the 44th IEEE Conference, Decision and Control (pp. 2278-2283), IEEE, 2005.

[3] Eid, R., Salimbahrami, B., Lohmann, B., Rudnyi, E. B., Korvink, J. G.: "Parametric order reduction of proportionally damped second order systems", Lehrstuhl für Regelungstechnik, TU München, 2006.

[4] Freund, R. W.: "Model reduction methods based on Krylov subspaces", Acta Numerica, 12, 267-319, 2003

[5] Benner, P., Feng, L.: "A robust algorithm for parametric model order reduction based on implicit moment matching", Springer, Cham, 2014.

[6] Blech, C., Appel, C. K., Ewert, R., Delfs, J. W., Langer, S. C.: "Numerical prediction of passenger cabin noise due to jet noise by an ultra–high-bypass ratio engine", J. of Sound and Vibration 464, 2020.

[7] Bodendiek, A., Bollhöfer, M.: Adaptive-order rational Arnoldi-type methods in computational electromagnetism. BIT Numerical Mathematics, 54(2), 357-380, 2014.